





Prototyping an Industrial Robot Arm for Deburring in Machining

^{1*}Yusuf Hamida El Naser, ²Gokhan Atali, ³Durmus Karayel, ⁴S.Serdar Ozkan,
¹Sakarya University of Applied Science Mechatronics Engineering

yusufelnaser@sakarya.edu.tr, 
gatali@sakarya.edu.tr, 

dkarayel@sakarya.edu.tr, 
sozkan@sakarya.edu.tr, 

Research Paper

Arrival Date: 05.08.2019

Accepted Date: 18.02.2020

Abstract

Deburring after production is an important problem for machining, casting and plastic forming in the manufacturing sector. The main subject of this study is to design a deburring robot arm. In the study, deburring operation has been performed by integrating a deburring tool at the end of the robot arm. To control the trajectory of deburring tool and optimum deburring force are two critical situations in such a special robot arm design. Since the parts that need to be cleaned are often not of uniform geometry and so the distribution of the burr and trajectory of robot arm will not uniform. Therefore, the robot arm that can follow this trajectory must have enough degrees of freedom. On the other hand, the cutting force between the deburring tool and the work piece and the magnitude of the normal force is also important. This force must be small so that it will not affect the structural rigidity of the arm and not damage the part and at the same time it must be big enough for deburring. This robot arm designed for deburring can also be used for industrial purposes when parameters are changed.

Keywords: Robot arm, Deburring, Machining

1. INTRODUCTION

Nowadays, even in high-tech machines, especially in machining, a burr-free manufacturing is often not possible. On the other hand, the burr is a risky formation both in terms of production quality and environmental damage. In addition to that, the burred parts not only cause problems in the assembly process, but also negatively affect the fatigue life. Numerous scientific studies have been carried out to optimize the process parameters in production to reduce burrs. However, it is still not possible to produce a completely deburred part. For this reason, the sensitive parts need to be subjected to an additional deburring process. This means an additional cost in production. A study in Germany reveals that the share of deburring costs in production costs is about 9% [1]. Since the method used for deburring directly affects the cost of production, many studies have focused on reducing this additional cost. Furthermore, deburring using conventional methods results in other problems, such as lack of safety, not being able to achieve the desired cleaning of parts in complex geometries, as well as cost. The use of robot technology for this process significantly reduces these problems. However, the robot to be designed must have special features for that tasks. It is important that the trajectory tracked by the cleaning tool manipulated by the robot and the contact force between the tool and the part

being cleaned can be controlled. For this purpose, studies on robotic arm design are remarkable in recent years. Ziliani et al. Have developed a 2-degree-of-freedom SCARA robot for deburring planar surface parts. The robot they developed is based on a force / speed based hybrid control algorithm. Although they successfully perform force and torque control in their work, there is no declaration of robot design [2]. Valente and Oliveira have proposed a new approach to tool path control in robotic deburring operations. In their study, they developed a correlation between the force value required to remove the burr and the tool path position and used the correlation they developed to control the system. In their systems, there is no robot that has been designed in a similar way since an ABB robot used as the manipulator [3]. In another study, they have developed an adaptive robotic system to correct position errors in castings and also to remove burrs. In this study, the dimensions of the workpiece surface were measured with the laser sensor in three dimensions and compared with the nominal dimensions and the excesses in the resulting faulty regions were eliminated [4]. Most of the relevant researchers have tried to develop different control algorithms for more precise deburring than existing systems [5-7]. In deburring, the control of the contact force between the tool and the workpiece is very important. This is because the excessive force will cause dimensional damage on the part, while the insufficient

*Corresponding Author: Sakarya Uygulamalı Bilimler Üniversitesi Mekatronik Mühendisliği, yusufelnaser@sakarya.edu.tr 0264 295 70 79

Bu çalışma ISITES2017'de sunulan bildiriden türetilmiştir.

contact force will not adequately remove the burr. For this reason, some researchers have focused on the control of contact force [8-13]. In the studies carried out on the subject, the hardware and control system mostly used is based on traditional technology. However, the point reached today in hardware, software, control algorithm and information technologies for the solution of the problem has brought many possibilities and ease. In contrast to other studies, the design of the robot arm is based on the creation of a prototype for the solution of the problem using new generation hardware, software and control technologies. In the study, firstly the formation of burrs and cleaning process are explained in general and then the design of the robotic arm for this purpose is started. Then, position control and force control were analyzed separately and the control system was designed. In the first part of the study, the studies in the literature are compared with the study conducted by the author. In the second part, the burr formation and the cleaning of the burrs are touched and in the third part, the workspace and kinematic equations of the designed robot arm are given. In the fourth chapter, the concepts of trajectory planning and force control are explained briefly and in the last chapter the results and the points that can be improved are discussed.

2. BURR FORMATION AND DEBURRING

In all production processes, burrs occur as an undesirable formation. Despite many efforts to eliminate the burr, a burr-free production is almost impossible, and more or less burring occurs. Especially in the production of sensitive systems, burr is a very important problem and needs to be cleaned. On the other hand, burrs are formed in many different forms according to production type, material properties, cutting tool geometry and process parameters. The resulting burr forms for different machining processes are shown in Figure 1 and some tools used to clean them are shown in Figure 2. Deburring is usually done manually using various tools. However, mechanical deburring systems have been developed especially for products manufactured by mass production. However, each of these systems is for one certain type of burr and does not have the flexibility to be adapted to another type.

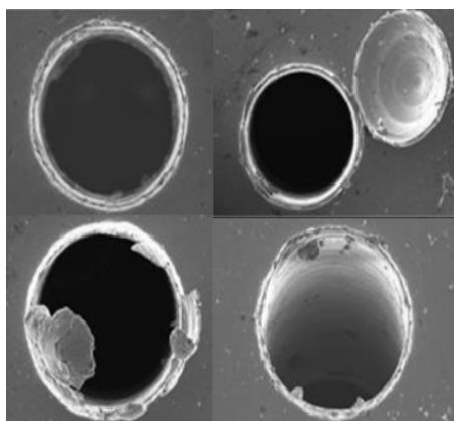
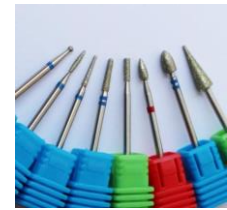


Figure 1. Burr formation in drilling



Manual deburring tools



Automatic deburring tools

Figure 2. Deburring tools

Therefore, it is not possible to develop a mechanical deburring system that can address all types of burrs of this very different geometric nature and structure. To meet this need, the Robotic Deburring System stands out as the only flexible system that can adapt itself to variable situations.

In recent years, studies in this direction have come into question and the issue is still up to date. This study aims to design an industrial robot arm in order to contribute to solution of this problem. This initial work is a prototype and is generally designed to deburr parts with prismatic geometry. However, by changing the parameter values used in the design, it can be used professionally for other production methods.

3. DESIGN OF THE ROBOT ARM

The designed robot arm has 3 degrees of freedom and features articulated manipulators. The robot arm consists of a motor rotating about the Y axis and 2 motors rotating about the Z axis and the chassis assembly connecting them together. The frame is designed to have a 40 mm axis offset between the first and second joints to avoid singularities. Thus, smooth and repeatable movement of the system is provided. Dynamixel AX-12A intelligent servo motors and Dynamixel Bioloid chassis components are used in the system. Figure 3 shows the movement axes of the robot arm. In the kinematic calculations of the arm, the deburring tool to be used was represented by cutting and sharpening the end points of the end member.

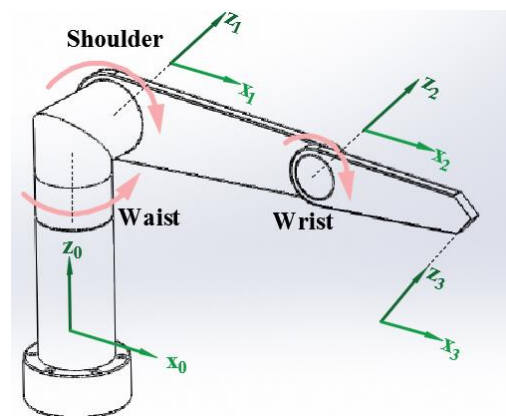


Figure 3. Axial representation of robot arm

3.1. Determination of the Limb Dimensions of the Robot Arm

The limb sizes of the robot arm are determined by the desired working area and the geometry to be machined within this area. In this study, the working area of the robot is 400 x 400 mm and the vertical distance from the base is $\ell = 100$ mm. The robot arm lengths determined according to the working area are presented in Figure 4.

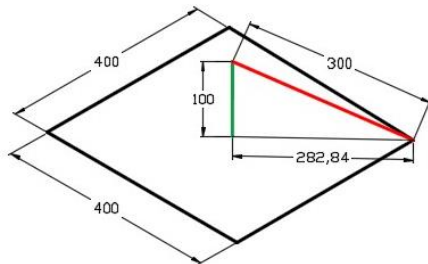


Figure 4. Illustration of robot arm lengths (mm)

When the robot arm is placed in the center of the working area, the sum of the second and third limb lengths (a, b) can be found as shown in equation 1.1;

$$a + b = \left(\left(\frac{400}{2} \right)^2 + \left(\frac{400}{2} \right)^2 + 100^2 \right)^{0.5} = 300 \text{ mm} \quad (1.1)$$

at least.

This value is the minimum value of the sum of the second and third limbs. If we show the second limb as a, the third limb as b, the inequality is obtained as in equation 1.2;

$$a + b \geq 300 \text{ mm} \quad (1.2)$$

In this case, limb lengths can be arbitrarily selected so that their sum does not fall below 300, and access to the boundaries of the working area of the arm can be made possible, but it should not be ignored that a dead zone as much as the distance between the limb lengths will arise. Therefore, limb lengths should be chosen as close as possible to each other.

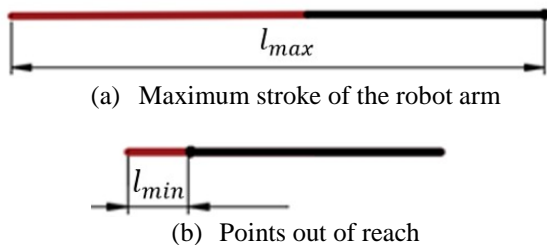


Figure 5. Robot arm reaching points

As a result of the above calculations, the 2nd limb length is selected as 160 mm and the 3rd limb length is 140 mm.

3.2. Kinematic Equations

3.2.1. Obtaining Forward Kinematics Equations

Denavit-Hartenberg methods were used in the analysis of forward direction kinematics of the robot arm. Accordingly, the D-H table obtained after the placement of the axis parameters is given in Table 1.

Table 1. Denavit-Hartenberg parameters

D-H	a_{i-1}	α_{i-1}	d_i	θ_i
0→1	0	90	$-\ell$	θ_1
1→2	0	-90	0	θ_2
2→3	a	0	d	θ_3
3→4	b	0	0	0

The parameters a,b,c,d were selected as a=160, b=140, $\ell=100$ and d=40 mm. Transformation matrices are given below.

$${}^0_1T = \begin{bmatrix} c\theta_1 & -s\theta_1 & 0 & 0 \\ 0 & 0 & -1 & 0 \\ s\theta_1 & c\theta_1 & 0 & 0 \\ 0 & 0 & 0 & 1 \end{bmatrix} \quad (2.1a)$$

$${}^1_2T = \begin{bmatrix} c\theta_2 & -s\theta_2 & 0 & 0 \\ 0 & 0 & 1 & 0 \\ -s\theta_2 & -c\theta_2 & 0 & 0 \\ 0 & 0 & 0 & 1 \end{bmatrix} \quad (2.1b)$$

$${}^2_3T = \begin{bmatrix} c\theta_3 & -s\theta_3 & 0 & a \\ s\theta_3 & c\theta_3 & 0 & 0 \\ 0 & 0 & 1 & d \\ 0 & 0 & 0 & 1 \end{bmatrix} \quad (2.1c)$$

$${}^3_4T = \begin{bmatrix} 0 & 0 & 0 & b \\ 0 & 0 & 0 & 0 \\ 0 & 0 & 1 & 0 \\ 0 & 0 & 0 & 1 \end{bmatrix} \quad (2.1d)$$

Accordingly, when the homogeneous transformation matrices (HTM) are formed and multiplied respectively, $s\theta$ and $c\theta$ represents $\sin\theta$ and $\cos\theta$, from base to end effector HTM is given in equation 2.1, robot tool coordinates are given in equation 2.2 and angle formulas are given in equations 2.3 and 2.4.

3.2.2. Obtaining Inverse Kinematics Equations

Obtaining inverse kinematic equations allows the burr cleaner to determine the angle values that the motors must rotate in order to perform work by hovering over the workpiece whose coordinates are known. These required angle values were found graphically and then transferred to LabVIEW environment to communicate with the motors. There are many studies on inverse kinematics subject in the literature [14, 15].

3.2.2.1. Obtaining the angle of 1st axis

The parameters used to find the first axis angle values are shown in Figure 6. If the projection point P_x and the projection z on the x-axis of the desired point to be reached are called, the values $a = 160$, $b = 140$, $l = 100$, $d = 40$ mm symbolized above;

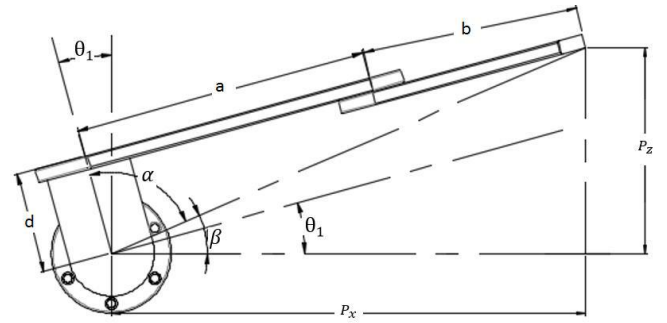


Figure 6. Inverse kinematics parameters of 1st axis

$${}^0T_4 = \begin{bmatrix} r_{11} & r_{12} & r_{13} & a * c \theta_1 * c \theta_2 - d * s \theta_1 - b * c \theta_1 * s \theta_2 * s \theta_3 + b * c \theta_1 * c \theta_2 * c \theta_3 \\ r_{21} & r_{22} & r_{23} & a * s \theta_2 + b * c \theta_2 * s \theta_3 + b * c \theta_3 * s \theta_2 + l \\ r_{31} & r_{32} & r_{33} & a * c \theta_2 * s \theta_1 + d * c \theta_1 - b * s \theta_1 * s \theta_2 * s \theta_3 + b * s \theta_1 * c \theta_2 * c \theta_3 \\ 0 & 0 & 0 & 1 \end{bmatrix} \tag{2.1}$$

The robot arm end effector coordinates are;

$$\begin{aligned} P_x &= 160 * c \theta_1 * c \theta_2 - 40 * s \theta_1 - 140 * c \theta_1 * s \theta_2 * s \theta_3 + 140 * c \theta_1 * c \theta_2 * c \theta_3 \\ P_y &= 160 * s \theta_2 + 140 * c \theta_2 * s \theta_3 + 140 * c \theta_3 * s \theta_2 + 100 \\ P_z &= 160 * c \theta_2 * s \theta_1 + 40 * c \theta_1 - 140 * s \theta_1 * s \theta_2 * s \theta_3 + 140 * s \theta_1 * c \theta_2 * c \theta_3 \end{aligned} \tag{2.2}$$

$$\alpha = \arctan2 \left(\frac{\sqrt{P_x^2 + P_z^2 - d^2}}{d} \right), \tag{2.3}$$

$$\beta = \arctan2 \left(\frac{P_z}{P_x} \right), \tag{2.4}$$

$\theta_1 = \alpha + \beta - \frac{\pi}{2}$ parametric value is obtained by simple geometric approach.

3.2.2.2. Obtaining angles of 2nd and 3rd axis

The parameters used to find the second and third axis angle values are presented in Figure 7.

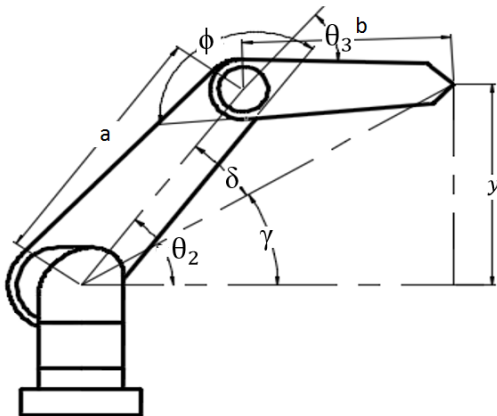


Figure 7. Inverse kinematics parameters of 2nd and 3rd axis

If the perpendicular distance of the second and third axes to each other on the Y axis is symbolized by y , the corresponding angle values can be found in equations 3.1, 3.2, 3.3 and 3.4;

$$\gamma = \arctan2 \left(\frac{y}{\sqrt{P_x^2 + P_z^2 - d^2}} \right), \tag{3.1}$$

$$\delta = \arccos \left(\frac{P_x^2 + P_z^2 - d^2 + y^2 + a^2 - b^2}{2 * a * \sqrt{P_x^2 + P_z^2 - d^2 + y^2}} \right), \tag{3.2}$$

$$\theta_2 = \gamma + \delta, \tag{3.3}$$

$$\phi = \arccos \left(\frac{-P_x^2 - P_z^2 + d^2 - y^2 + a^2 + b^2}{2 * a * b} \right), \tag{3.4}$$

$\theta_3 = \pi - \phi$ respectively.

The program interface used to transfer inverse kinematic equations to the LabVIEW environment is shown in Figure 8.

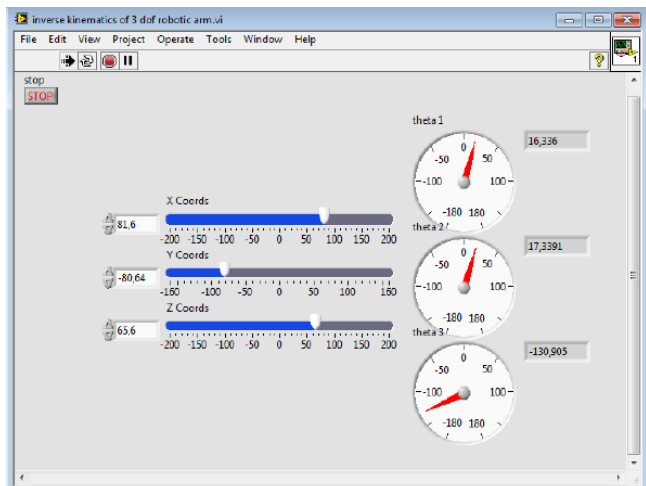


Figure 8. LabVIEW interface for inverse kinematic equations

4. DESIGN OF CONTROL SYSTEM

In the robotic arm designed for deburring, the design of the control system is mainly based on position control and force control. The deburring tool must follow the respective edges of the part to be cleaned. This is only possible by determining the path to be cleaned, i.e. the trajectory and controlling the tool to follow the trajectory. Another critical situation is the cutting force that occurs at the point of contact with the deburring tool. As a result of this excessive force, the tool will damage the part together with the burr and will cause a part called negative chips, causing the part to break down. If the cutting force is lower than necessary, the burr will not be sufficiently cleaned. Therefore, an optimum force must be applied, and this is only possible by controlling the force.

4.1. Position Control

4.1.1. Determination of the Trajectory

The robots are capable of repeating the trajectory that has been introduced to them once. What is essential here is the precise and accurate identification of the trajectory to be monitored and the control of its position. This position control and determination of the trajectory to be followed is an important issue in robotic applications. There are many parameters such as part geometry to be processed, physical limitations of robot chassis and complexity of the process to be applied. For example, when moving and sorting from one point to another within an empty work area, it is sufficient to know the coordinates of the two points from which the part is received and the part to be left. On the other hand, the modeling of the motion between these two points is often not important, but in industrial applications such as welding, deburring and dyeing, the geometry of the workpiece is continuously monitored as a route [16]. In this application, the trajectory is realized by determining the edges of the workpiece to be deburred by means of CAD file and coordinating these edges with the help of LabView program

and passing these coordinates in a series of inverse kinematic equations respectively to find the necessary motor angles. In this trajectory, it is ensured that the contact between the burr cleaner and the workpiece is smooth and continuous and the non-contact between the burr cleaner and the burr cleaner can be prevented as a result of changing the force applied to the workpiece.

4.2. Force Control

4.2.1. Determination of the Optimal Force

Deburring is carried out by applying a force to the deburring workpiece along the trajectory determined by position control with the deburring tool placed on the robot arm. The magnitude of the force varies according to the torque value produced by the motors used in the robot arm system, the density of the burr to be cleaned from the workpiece, the material of the workpiece and the deburring cleaner, the contact surface and geometry of the cleaner and the workpiece. [17] Therefore, it is necessary to maintain this force which will act normally and along the surface to clean the burr, and to maintain it at the optimum intervals determined. The force must be greater than the minimum force required for deburring on the workpiece, but also less than the maximum force that will not exceed the depth of burr desired to be cleaned and will not damage the workpiece and the cleaning tool [3]. Accordingly, the limits of the shear forces corresponding to the various types, dimensions and characteristics of the burrs are determined and compared with the feedback received in real time from the force sensor placed on the burr removal tool. When the maximum value of the specified range is exceeded, the deburring tool moves away from the contact surface until it reaches a value between the force limits, and when it falls below the minimum value, it approaches the contact surface.

5. RESULTS AND FUTURE WORKS

In this study, a robot arm design which is used for deburring is presented. The CAD model of the part to be cleaned was used to determine the trajectory to be followed by the deburring tool and this trajectory was used for position control. The interaction between the tool and the workpiece directly affects the cutting force. For this reason, a special deburring tool is used to obtain optimum force ranges by providing the necessary flexibility. Essentially, this team itself is a mechatronic system. Because, apart from the tool which performs the cutting process, it also includes a motor to provide cutting movement and a force sensor in which force measurement is performed. This robot arm, designed for deburring purposes, is a prototype and can be used for industrial purposes when the values of the parameters are changed. On the other hand, this study has the potential to form the basis for further studies. In the next study, artificial intelligence methods will be used to determine the type of burr as a result of detection of burr form and size by image processing method. In addition, the selection and replacement of the deburring tool for the specified burr type

will be performed automatically. In this way, it will be possible to perform all operations such as detection, analysis of burr form, selection of appropriate cleaning tool and necessary parameters by the developed system.

6. ACKNOWLEDGEMENTS

This study was supported by Sakarya University Scientific Research Projects Commission with the name "Industrial Purpose Robot Arm Design and Production" within the scope of Master Thesis Projects numbered 2017-50-01-009.

7. REFERENCES

- [1] L. Leitz, V. Franke, and J.C. Aurich, Burr Formation in Drilling Intersecting Holes, Proceedings of the CIRP International Conference on Burrs, 2009; 109-115.
- [2] G. Ziliani, A. Visioli, G. Legnani, A mechatronic approach for robotic deburring, *Mechatronics* 17, 2007; 431–441.
- [3] Carlos M. O. Valente, João F. G. Oliveira, A New Approach For Tool Path Control In Robotic Deburring Operations, ABCM Symposium Series in Mechatronics, 2004; 124-133.
- [4] Hubert Kosler, Urban Pavlovčič, Matija Jezeršek, Janez Možina, Adaptive Robotic Deburring of Die-Cast Parts with Position and Orientation Measurements Using a 3D Laser-Triangulation Sensor, *Strojniški vestnik - Journal of Mechanical Engineering* 62, 2016; 207-212.
- [5] H. Kazerooni, J. J. Bausch, B. M. Kramer, An Approach to Automated Deburring by Robot Manipulators, *Transactions of the ASME* 108, 1986; 354-359.
- [6] M. G. Her, H. Kazerooni, Automated Robotic Deburring of Parts Using Compliance Control, *Transactions of the ASME* 113, 1991; 60-66.
- [7] Fusaomi Nagata, Tetsuo Hase, Zenku Haga, Masaaki Omoto, Keigo Watanabe, CAD/CAMbased position/force controller for a mold polishing robot, *Mechatronics* 17, 2007; 207–216.
- [8] Thomas M. Stepien, Larry M. Sweet, Malcolm C. Good, Masayoshi Tomizuka, Control of Tool/Workpiece Contact Force with Application to Robotic Deburring, *IEEE Journal Of Robotics And Automation*, 1987; 7-18.
- [9] G. M. Bone, M. A. Elbestawi, R. Lingarkar, L. Liu, Force Control for Robotic Deburring, *Journal of Dynamic Systems, Measurement, and Control* 113, 1991; 395-400.
- [10] J. Norberto Pires, J. Ramming, S. Rauch, R. Araújo, Force/Torque Sensing Applied to Industrial Robotic Deburring Control for Robotic Deburring, *Sensor Review* 22, 2002; 232 – 241.
- [11] G. M. Bone, M. A. Elbestawi, Robotic force control for deburring using an active end effector. *Robotica*, 7(4), 1989; 303-308.
- [12] M. H. Liu, Force-controlled fuzzy-logic-based robotic deburring. *Control engineering practice*, 3(2), 1995; 189-201.
- [13] K. Kiguchi, T. Fukuda, Position/force control of robot manipulators for geometrically unknown objects using fuzzy neural networks, *IEEE Transactions on Industrial Electronics*, 47(3), 2000; 641-649.
- [14] S. Kucuk, Z. Bingul, Inverse kinematics solutions for industrial robot manipulators with offset wrists. *Applied Mathematical Modelling*, (7-8), 2014; 1983-1999.
- [15] S. Kucuk, Z. Bingul, The inverse kinematics solutions of fundamental robot manipulators with offset wrist, *IEEE-International Conference of Mechatronics*, 2005; 197-202.
- [16] A. Sokolov, Robot motion realisation using LabVIEW, *Periodica Polytechnica. Engineering. Mechanical Engineering*, 1999; 43(2), 131.
- [17] S. Malkin, Grinding technology. Theory and applications of machining with abrasives. Ellis Horwood Limited, England; 1989.